ELSEVIER

International Journal of Mass Spectrometry 210/211 (2001) 591–602

www.elsevier.com/locate/ijms

Structural characterization of hyperbranched polyesteramides: MS^n and the origin of species

Sander Koster[a], Chris G. de Koster[b], Rolf A.T.M. van Benthem[b],
Marc C. Duursma[a], Jaap J. Boon[a], and Ron M.A. Heeren[a,*]

[a]*Unit for Macromolecular Mass Spectrometry, FOM-Institute for Atomic and Molecular Physics, Kruislaan 407, 1098 SJ, Amsterdam, The Netherlands* [b]*DSM Research, P.O.Box 18, 6160MD Geleen, The Netherlands*

Received 14 December 2000; accepted 28 January 2001

Abstract

Four hyperbranched synthetic polyesteramides were synthesized by the polycondensation of the trifunctional diisopropanolamine (D) and difunctional anhydrides (X) of succinic acid, glutaric acid, 1,2-cyclohexane dicarboxylic acid, and phthalic acid. The polymers were analyzed with electrospray ionization Fourier transform ion cyclotron resonance mass spectrometry. The most intense oligomer series observed was X_nD_{n+1} containing diisopropanolamine end groups as expected from the polycondensation conditions. A series of oligomers X_nD_{n+1}–H_2O is observed as well, which can have its origin in the polymerization process or alternatively could result from in-source fragmentation of X_nD_{n+1}. Breakdown diagrams of the protonated parent ions X_3D_4 and additional MS^n (n = 1, 2, 3) measurements gave insight in the fragmentation behavior of the polymers. Three main fragmentation pathways have been observed for all polymers of which the loss of H_2O to oxazolonium ions has the lowest onset energy followed by the rearrangement of the amide and ester bonds also leading to oxazolonium ions. The loss of a second H_2O to allylic or morpholine end groups has highest onset energy. MS^3 experiments demonstrated that the presence of a series of oligomers X_nD_{n+1}–H_2O can be attributed to the polymerization process. Most probably an allylic end group has formed from one of the alcohol end groups. The formation of allylic end groups partly terminates the polymerization reaction and results in a change of the composition of the molecular weight distribution and decrease of the number average molecular weight. (Int J Mass Spectrom 210/211 (2001) 591–602) © 2001 Elsevier Science B.V.

1. Introduction

Soft ionization techniques for synthetic polymer characterization like matrix-assisted laser desorption ionization (MALDI) and electrospray ionization (ESI) have become widely used in mass spectrometry mainly because intact protonated or cationized molecular ions are generated [1–6]. This makes a determination of the monomer and end group mass by linear regression easy [7–9]. Sequence information of copolymers can be obtained with postsource decay (PSD) and collisionally activated dissociation (CAD) studies in sector and time-of-flight instruments and ion traps like Fourier transform ion cyclotron resonance (FTICR) [10–12]. Most studies concern linear polymers although some branched polymers have been successfully analysed [13–17]. An example of a

---

* Corresponding author. E-mail: heeren@amolf.nl

1387-3806/01/$20.00 © 2001 Elsevier Science B.V. All rights reserved
PII S1387-3806(01)00416-X

recent mass spectrometric study of a branched polymer (de Koster and Nibbering [15]) concerns a hyperbranched polyesteramide synthesized by the polycondensation of the trifunctional diisopropanolamine (D) and the difunctional hexahydrophthalic acid anhydride (C) [15,18,19]. Extensive in-source decay was observed for ions generated by field desorption (FD) and MALDI for this particular branched polymer. These fragments appear in the spectra as C_nD_{n+m}–H_2O ($m=0$–2) ions showing that MALDI and FD are not as soft as is often stated. Metastable decay of the parent ion upon PSD without a collision gas was also observed for the MALDI generated ions. This resulted in the rearrangement of the amide and ester bonds to oxazolonium ions, which appear in the spectra as C_nD_{n+m}–H_2O ($m=0$–1) ions. For ESI generated ions, the intensity of the oligomeric ions C_nD_{n+m}–H_2O ($m=0$–1) relative to the intensity of the intact molecular ions C_nD_{n+m} ($m=0$–1) was lowest. It was however not possible to determine whether the low intensity peaks C_nD_{n+m}–H_2O ($m=0$–2) were generated in the ESI source or during the polymerization reaction. The ion series observed in ESI can hence have a mixed origin that cannot be distinguished exclusively by the determination of their *m/z* values.

From a polymer synthesis point of view, it is important to know whether the C_nD_{n+m}–H_2O ($m=0$–2) series is generated in the polymerization reaction or by in-source fragmentation upon ESI. The generation of this oligomer series C_nD_{n+m}–H_2O ($m=0$–2) during the polymerization implies that some of the functional groups of the oligomers have terminated by allylic end group formation which influences the composition of the molecular weight distribution. With MS^n studies the origin of the oligomer series C_3D_4–H_2O has been determined. At first, the fragmentation behavior of the protonated oligomer C_3D_4 has been studied by energy resolved MS^2 collisionally activated dissociation experiments. The information obtained from this study is used to interpret MS^3 experiments which are necessary to determine the origin of the oligomer series C_3D_4–H_2O. This study has been performed for four hyperbranched polyesteramides, which were synthesized by the polycondensation of an excess of the trifunctional diisopropanolamine and the difunctional anhydrides of succinic acid, glutaric acid, 1,2-cyclohexane dicarboxylic acid and phthalic acid.

2. Materials and methods

2.1. ESI FTMS analysis

The measurements were performed on a modified FTICR-MS (Bruker-Spectrospin APEX 7.0e, Fällanden, Switzerland) [20,21] equipped with an ESI source [9]. The cell was an in house constructed open cell, which will be extensively described in another communication [22]. Pulsed gas trapping with argon at $P_{\mathrm{Ar}}=5.2\times10^{-6}$ mbar for 2 s was used to enhance trapping of the ions in the open cell. On-resonance excitation collisionally activated dissociation in the ion cyclotron resonance (ICR) cell was used to activate the parent ions generated by electrospray. Argon was used as collision gas ($P_{\mathrm{Ar}}=5.2\times10^{-6}$ mbar). The geometry factor α of the open cell necessary for the calculation of the excitation potentials on the excitation electrodes was estimated to be 1 based on a comparison between room temperature breakdown diagrams of several peptides. The peak-to-peak voltage of the excitation rf excitation signal was in all CAD experiments 17.6 V. The procedure followed for the construction of breakdown diagrams and calculation of the center of mass collision energy $E_{\mathrm{kin,com}}$ has been described earlier [23]. For the energy resolved experiments, three scans were summed at each point of collision energy.

2.2. Hyperbranched polyesteramides

The hyperbranched polyesteramides used for this study are polycondensation products of the trifunctional diisopropanolamine (D) and a difunctional dicarboxylic acid anhydride provided by DSM (Geleen, The Netherlands). The difunctional dicarboxylic acid anhydrides used in the polymerisations are succinic acid anhydride (S), glutaric acid anhydride (G), phthalic acid anhydride (P), and 1,2-

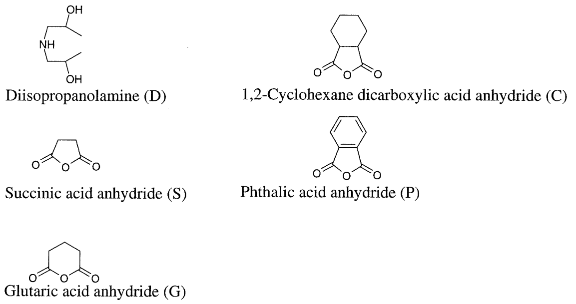

Fig. 1. Structure of the di- and trifunctional monomers for the synthesis of the hyperbranched polyesteramides.

cyclohexane dicarboxylic acid anhydride (C). Fig. 1 shows the structures of the monomers. The synthesis is described in detail by van Benthem et al. for 1,2-cyclohexane dicarboxylic acid anhydride [18]. The other polymers were synthesized in a similar manner. The products of the polycondensation reactions of the anhydrides of succinic acid, glutaric acid, phthalic acid, and cyclohexane dicarboxylic acid have a designed number average molecular weights of 1200, 1200, 1000, and 925, respectively [18]. The spray solutions consist of 74:24:2 methanol (Merck, Darmstadt, Germany):H_2O:HAc (Biosolve, Valkenswaard, The Netherlands) in which approximately 300 μg/mL of the hyperbranched polymers is dissolved.

3. Results and discussion

The hyperbranched polyesteramides were all produced by the same synthetic route, in which the trifunctional monomer diisopropanolamine (D) was added in excess to the dicarboxylic acid anhydride. The notation used to denote the dicarboxylic acid anhydrides is S, G, C, and P for the anhydrides of succinic acid, glutaric acid, 1,2-cyclohexane dicarboxylic acid and phthalic acid, respectively. Fig. 2 shows the mass spectrum of the phthalic acid based polymer. The spectrum reveals the presence of a series of protonated and sodiated polyesteramide oligomers although sodium salts were not added to the spray solution. End group analysis shows that the

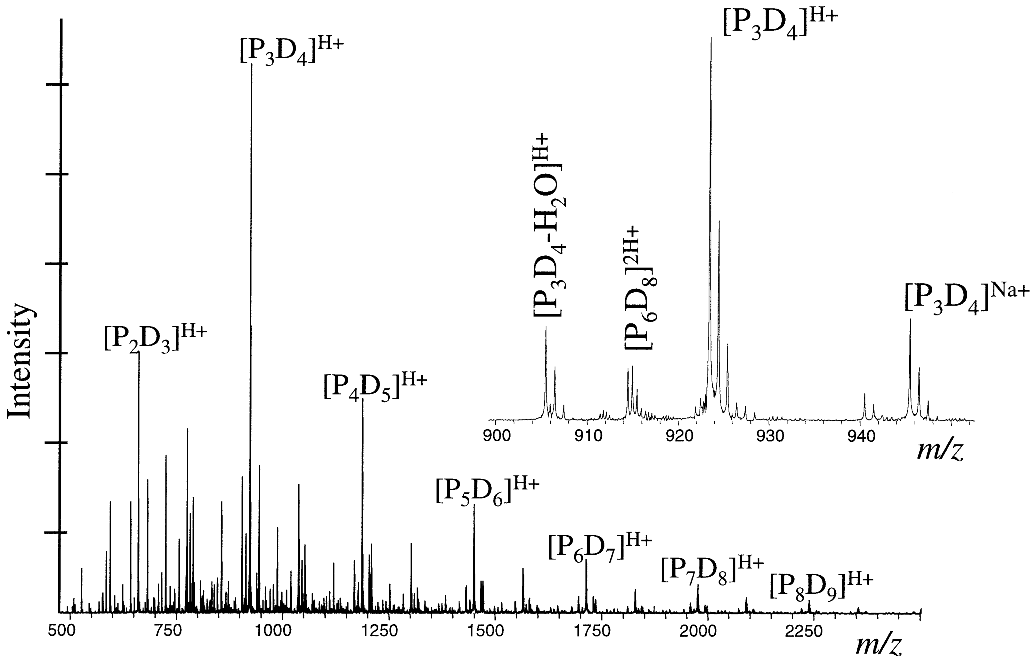

Fig. 2. ESI FTMS mass spectrum of the phthalic acid based hyperbranched polyesteramide.

most intense oligomers P_nD_{n+1} and P_nD_{n+2}, contain diisopropanolamine end groups. The n denotes the number of monomers in a given oligomer. Cyclic oligomers P_nD_n were also observed. The oligomer series P_nD_{n+2} are formed by the reaction of an oxazolonium ion, created in the polymerization reaction [15], with an amine. The polymerization conditions were chosen such that the concentration of amine groups during the polymerization was low [15] and the concentration of P_nD_{n+2} in the final polymer was lower than the concentration of P_nD_{n+1}. The oligomer series observed in the mass spectra of the other hyperbranched polyesteramides are very similar to figure 2 (spectra not shown). A detailed mass spectrometric study of the composition and structure of the hyperbranched polyesteramides will be published elsewhere.

Series of oligomers P_nD_{n+1}–H_2O, P_nD_{n+2}–H_2O and P_nD_n–H_2O have been observed for all polymers. The ions may be pseudomolecular ions of oligomers due to the polymerization process or may be due to fragmentation as a result of internal energy uptake in the ion source, ion transport section or ion trap. It is known from literature however that the 1,2-cyclohexane dicarboxylic acid anhydride based polymer undergoes metastable fragmentation for MALDI generated ions [15]. Whether similar processes are possible during ESI is not known and is the aim of the research described in this paper.

The most important fragmentation pathways of the hyperbranched polyesteramides and the energetics involved were studied by MS^n of the protonated oligomers containing three diacid anhydrides and four diisopropanolamines (S_3D_4, G_3D_4, C_3D_4 and P_3D_4). The insight obtained from these experiments was used to determine whether the oligomer series P_3D_4–H_2O, S_3D_4–H_2O, G_3D_4–H_2O, and C_3D_4–H_2O have their origin in the polymerization process or result from the mass spectrometer.

3.1. Glutaric acid anhydride based polymer

Only the loss of H_2O from $[G_3D_4]^{H+}$ with *m/z* 821 is observed for a relatively low center of mass collision energy ($E_{kin,com}$) of 0.3 eV (spectrum not shown). The notation $[G_3D_4]^{H+}$ is used instead of the more conventional $[G_3D_4{+}H]^+$ notation because this allows to distinguish protonated ions from oxazolonium ions (see the following discussions). The proposed mechanism for H_2O loss is the intramolecular transfer of the proton to one of the OH end groups, which results in the loss of H_2O and the formation of an oxazolonium ion as shown in Scheme 1 [24]. Note that the positive charge of the parent ion is a proton. The positive charge becomes a quartenary ammonium ion stabilized by oxazolonium ion formation for the fragment ion. In Fig. 3 the MS^2 spectrum obtained at a higher collision energy ($E_{kin,com}$=2.0 eV) is shown. Ten fragments are observed. Ions resulting from the loss of two water molecules are of low abundance and cannot be explained by the formation of two oxazolonium ions, since the parent ion is charged by only one proton. Ions due to the loss of the second water possibly originate from another OH end group on the parent ion resulting in an allylic or 2,6-dimethyl morpholine end group.

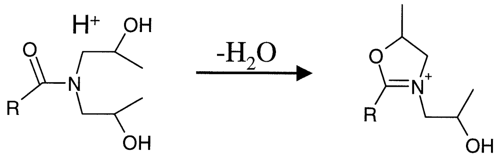

Scheme 1.

Two mechanisms are proposed in [15] that explain the unimolecular rearrangement of the amide and ester bond. The rearrangement of the amide and ester bonds are shown for the glutaric acid based polyesteramide in Schemes 2 and 3, respectively. Most fragments observed in Fig. 3 can be explained by these mechanisms. Stable oxazolonium ions, denoted by the addition of $^{ox+}$, are formed due to the rearrangement of the amide and ester bond $^e[G_2D_3$–$H_2O]^{ox+}$, $^b[G_2D_2$–$H_2O]^{ox+}$, $^e[GD_2$–$H_2O]^{ox+}$, and $^b[GD$-$H_2O]^{ox+}$. Rearrangements of the amide and ester bonds are denoted by *b* and *e* superscripts, respectively. The *b* notation that indicates the rearrangement of the amide, has its origin in the peptide literature where such *b* ions are very common. The nomenclature has also been introduced for polyester-

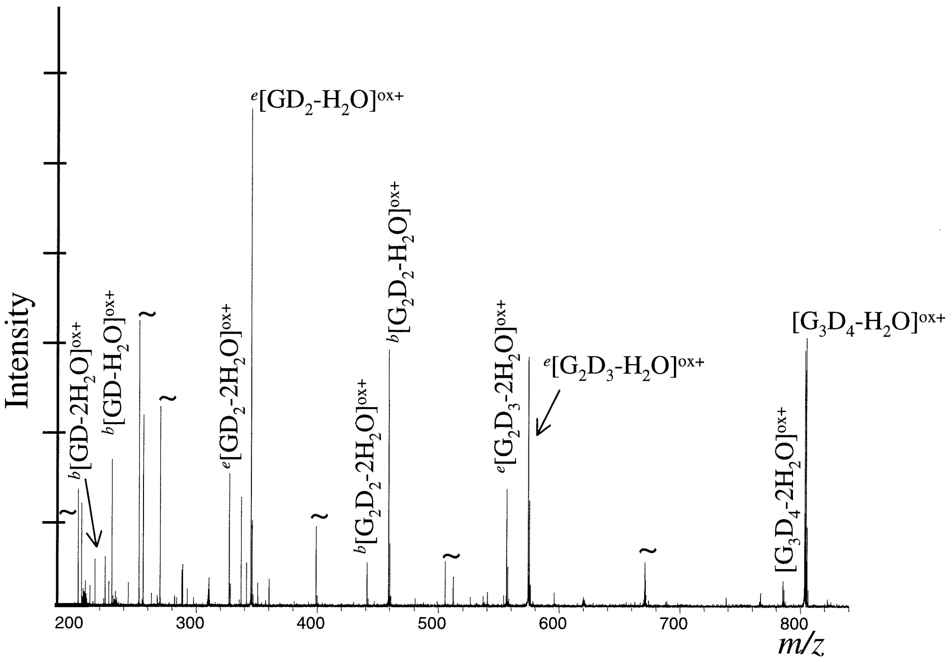

Fig. 3. MS/MS spectrum of $[G_3D_4]^{H+}$ at relatively high collision energy $E_{\mathrm{kin,com}} = 2.0$ eV. The tilde denotes electronic noise.

amides [15]. A series of fragments is observed that is due to oxazolonium ion formation followed by an additional H_2O loss. This results in the singly charged fragments $^{e}[G_2D_3–2H_2O]^{ox+}$, $^{b}[G_2D_2–2H_2O]^{ox+}$, $^{e}[GD_2–2H_2O]^{ox+}$, and $^{b}[GD–2H_2O]^{ox+}$. These fragments cannot be explained by the loss of H_2O by oxazolonium ion formation followed by a rearrangement by one of the two mechanisms shown in Schemes 2 and 3, because the charge state is one. It is therefore more probable that an ester or amide bond is rearranged to an oxazolonium ion followed by the loss of H_2O.

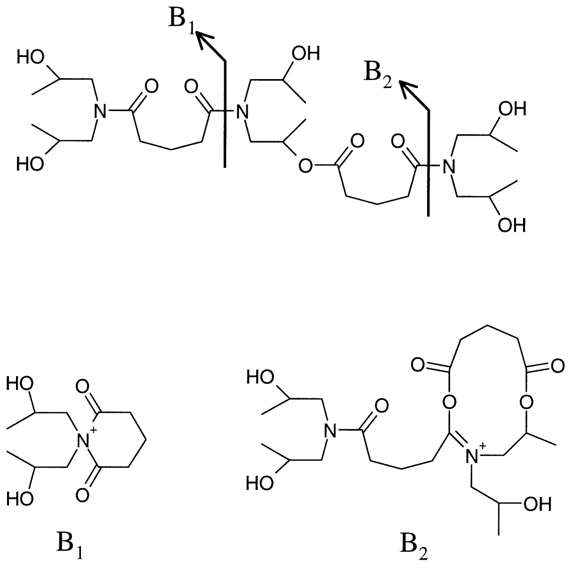

Scheme 2.

Note that only one fragment is observed as oxazolonium ion during the rearrangements and the other one is always a neutral fragment. This is usually not observed for pseudomolecular ions of polyesters with only ester bonds nor for peptides containing only amide bonds, where the appearance in the MS/MS spectrum depends on the proton or cation affinity of the fragments [12,25–27].

The MS/MS spectrum at $E_{\mathrm{kin,com}}=0.3$ eV is very different from the MS/MS spectrum at $E_{\mathrm{kin,com}}=2.0$ eV. Therefore the energy dependence of the dissociation of the parent ion is studied to gain insight in the relative strengths of the amide and ester bonds in the protonated polyesteramide oligomer. The collision energy dependence of the fragmentation

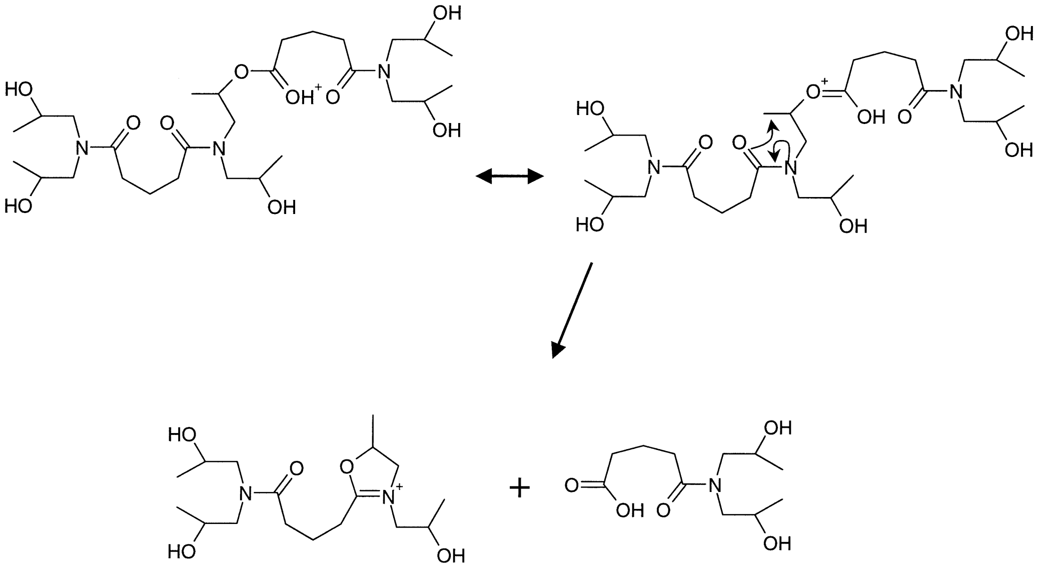

Scheme 3.

process is studied by constructing the breakdown diagram for the parent ion and fragments as shown in Fig. 4(a). The survival yield of the parent ion and the most intense fragments due to rearrangements of the ester and amide bonds, $^{e}[G_2D_3–H_2O]^{ox+}$, $^{b}[G_2D_2–H_2O]^{ox+}$, $^{e}[GD_2–H_2O]^{ox+}$, $^{b}[GD\text{-}H_2O]^{ox+}$, and ions due to the loss of H_2O are plotted as a function of the center of mass collision energy $E_{\mathrm{kin,com}}$. The survival yield of the parent ion is defined as the intensity of the parent ion divided by the sum of the intensities of the parent ion and all fragments. To obtain the survival yield of the fragments, the intensity of a particular fragment is divided by the sum of the parent ion and all fragment ions. Although only five fragment ions are shown in Fig. 4(a), all fragments observed have been used in the calculation of the survival yield. The reproducibility of the survival yield of the parent ion was about 5%. Fragments with *m/z* lower than 107 are not detected, but could influence the breakdown diagram.

Fig. 4(a) clearly demonstrates that the lowest energetic fragmentation pathway is the loss of H_2O from the OH end groups, which has an onset energy of $E_{\mathrm{kin,com}}=\sim0.3$ eV. The breakdown diagram shows that the fragments due to rearrangement of the amide and ester bonds do not appear at the same collision energies. The lines in the figure are used to guide the eyes. Rearrangements of the ester bonds, fragments $^{e}[G_2D_3–H_2O]^{ox+}$ and $^{e}[GD_2–H_2O]^{ox+}$, are observed at an onset energy of $E_{\mathrm{kin,com}}=\sim0.8$ eV, whereas the amide bonds starts rearranging at ~1.2 eV (fragments $^{b}[G_2D_2–H_2O]^{ox+}$ and $^{b}[GD–H_2O]^{ox+}$). The intensity ratio, of the fragments in the spectra, changes dramatically with the collision energy. For example, at center of mass collision energy $E_{\mathrm{kin,com}}=2.0$ eV the intensity of fragment $^{e}[G_2D_3–H_2O]^{ox+}$ is approximately the same as the intensity of fragment $^{e}[GD_2–H_2O]^{ox+}$. At a higher collision energy $E_{\mathrm{kin,com}}=3.8$ eV the intensity of $^{e}[GD_2–H_2O]^{ox+}$ becomes 3 times higher than $^{e}[G_2D_3–H_2O]^{ox+}$.

In Fig. 4(b) the breakdown diagram for the same parent ion $[G_3D_4]^{H+}$ is presented. Only fragments due to the loss of two H_2O molecules and amide bond rearrangements are shown for reasons of clarity. Fig. 4(c) shows the results obtained for the ester bonds. Ions due to the loss of two H_2O molecules (fragment ion $[G_3D_4–2H_2O]^{ox+}$) from the parent ion appear at significantly higher collision energy ($E_{\mathrm{kin,com}}=\sim1.4$ eV) than ions due to the loss of the first H_2O $[G_3D_4–H_2O]^{ox+}$. At

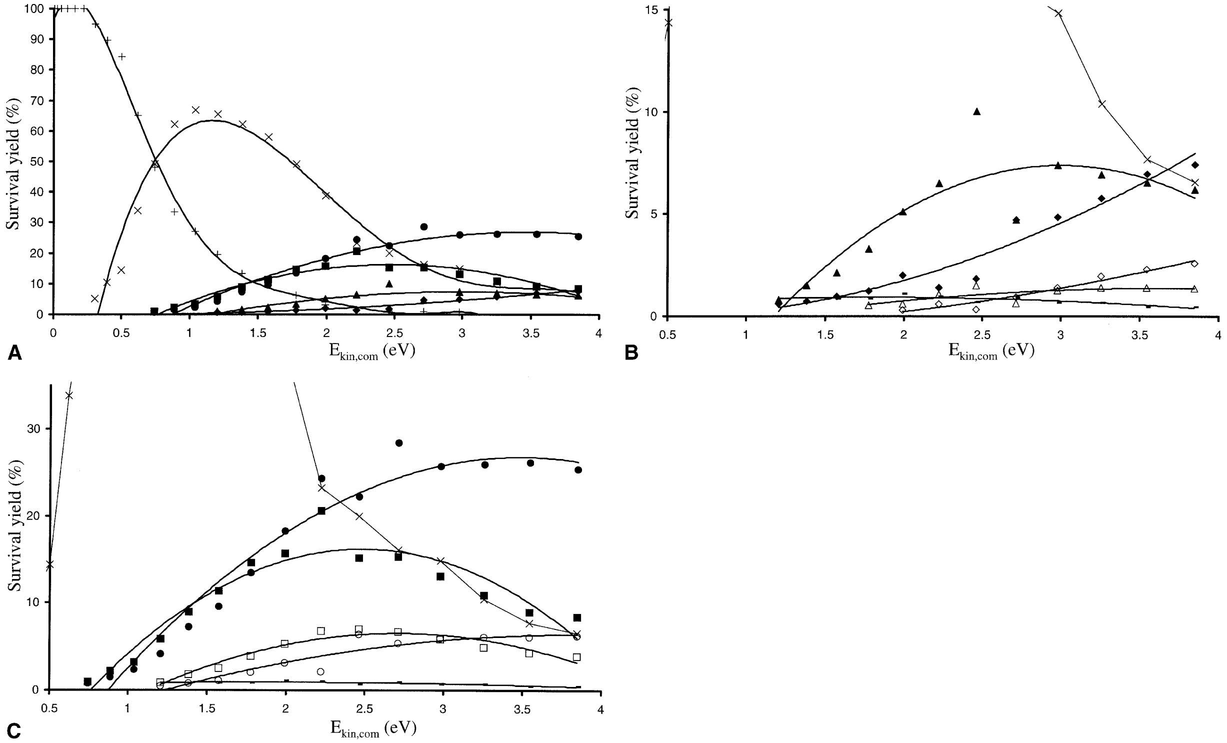

Fig. 4. Breakdown diagrams of G_3D_4+H]$^+$. For the most intense fragments $^e[G_2D_3–H_2O]^{ox+}$, $^b[G_2D_2–H_2O]^{ox+}$, $^e[GD_2–H_2O]^{ox+}$, $^b[GD–H_2O]^{ox+}$, and ions due to the loss of H_2O (a). Enlargements of breakdown diagram concerning amide bond rearrangements (b) and ester bonds (c). The fragments are denoted by a cross $[G_3D_4–H_2O]^{ox+}$, a dashed line $[G_3D_4–2H_2O]^{ox+}$, a closed square $^e[G_2D_3–H_2O]^{ox+}$, an open square $^e[G_2D_3–2H_2O]^{ox+}$, a closed triangle $^b[G_2D_2–H_2O]^{ox+}$, an open triangle $^b[G_2D_2–2H_2O]^{ox+}$, a closed circle $^e[GD_2–H_2O]^{ox+}$, an open circle $^e[GD_2–2H_2O]^{ox+}$, a closed diamond $^b[GD–H_2O]^{ox+}$ and an open diamond $^b[GD–2H_2O]^{ox+}$ and parent ion with a plus sign $[G_3D_4]^{H+}$. The lines are used to guide the eyes.

approximately the same collision energy where the second H_2O loss is observed, four fragments appear in the MS/MS spectra, which are due to rearrangements of the ester and amide bond with an additional loss of a H_2O. This results in singly charged fragment ions $^e[G_2D_3–2H_2O]^{ox+}$, $^b[G_2D_2–2H_2O]^{ox+}$, $^e[GD_2–2H_2O]^{ox+}$, and $^b[GD–2H_2O]^{ox+}$.

It is concluded from Fig. 4(a)–(c) that the three different fragmentation pathways observed can be distinguished by their onset center of mass collision energies. The formation of oxazolonium ions by the loss of H_2O has the lowest onset energy followed by the formation of oxazolonium ions by amide and ester rearrangement. The loss of the second H_2O, most probably by formation of allylic or 2,6-dimethyl morpholine end groups, has the highest onset energy.

3.2. Succinic and 1,2-cylohexane dicarboxylic acid anhydride based polymers

In the same way as the glutaric acid anhydride based polymer, the lowest energetic fragmentation pathway of the polyesteramides based on succinic acid anhydride is the loss of H_2O at $E_{kin,com} = \sim 0.25$ eV. The MS/MS spectra of $[S_3D_4]^{H+}$ (not shown) contain fragments due to the same mechanisms as observed in Fig. 3 for $[G_3D_4]^{H+}$. The main difference between the breakdown diagrams of $[S_3D_4]^{H+}$ and $[G_3D_4]^{H+}$ is that the difference in onset energy of the rearrangement of the ester ($E_{kin,com} = \sim 0.7$eV) and amide ($E_{kin,com} = \sim 0.5$ eV) bonds is reversed for $[S_3D_4]^{H+}$ with the exception of fragment ion $^b[SD–H_2O]^{ox+}$ with a $E_{kin,com} = \sim 1.8$ eV.

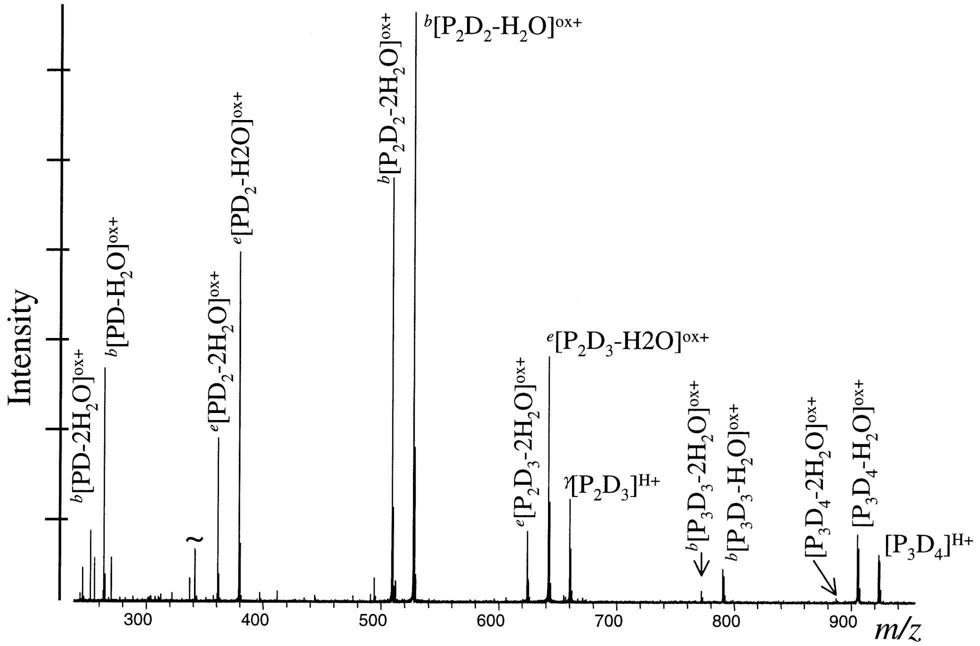

Fig. 5. MS/MS spectrum of $[P_3D_4]^{H+}$ m/z 923 at $E_{kin,com}=1.25$ eV.

For the 1,2-cyclohexane dicarboxylic acid anhydride based polymer a loss of one D unit by amide rearrangement to $^{b}[C_3D_3–H_2O]^{ox+}$ is observed as the lowest energetic fragmentation pathway together with the loss of H_2O to $[C_3D_4–H_2O]^{ox+}$ at $E_{kin,com}=\sim 0.3$ eV. The onset energies for the rearrangement of the ester and other amide bonds have approximately the same values as the collision energy of the ester bonds ($E_{kin,com}=\sim 0.4–0.9$ eV).

These results demonstrate that the onset energy for the ester and amide rearrangement strongly depends on the structure of the diacid anhydride and that this energy resolved experiment can be used to study the structure of the diacid anhydride. However, as observed for the glutaric acid anhydride based polymer, the onset energies for the three main fragmentation pathways have the following order: H_2O loss$<$ester and amide rearrangement$<2^{nd}$ H_2O loss.

3.3. Phthalic acid anhydride based polymer

The MS/MS spectrum of $[P_3D_4]^{H+}$ with m/z 923 in Fig. 5 shows two remarkable features. The first feature is an intense peak due to the loss of one diisopropanolamine resulting from an amide rearrangement $^{b}[P_3D_3–H_2O]^{ox+}$. This fragment was not observed for the polymers based on succinic acid anhydride and glutaric acid anhydride although it is connected to amide or ester bonds. The fragment was low in intensity in the case of the polymer based on 1,2-cylohexane dicarboxylic acid anhydride. A second feature is an intense peak at m/z 660, which cannot be explained by a rearrangement of the amide or ester bond. The mass difference between this fragment and fragment $^{e}[P_2D_3–H_2O]^{ox+}$ corresponds with H_2O indicating that the parent ion $[P_3D_4]^{H+}$ has lost one PD monomer to $[P_2D_3]^{H+}$. Such depolymerisating fragmentations were observed earlier for the copolyester poly(di-propoxylated bisphenol-A/isophthalic acid/adipic acid) for which a γ-hydrogen rearrangement was proposed [12]. Such a γ-hydrogen rearrangement can be used to explain the formation of $[P_2D_3]^{H+}$ also. This rearrangement must however lead to a protonated species $^{\gamma}[P_2D_3]^{H+}$ because the formation of an oxazolonium ion with composition P_2D_3 is structurally prohibited. The appearance of the fragments in the MS/MS spectra upon γ-hydrogen rearrangement depends on the proton affinity of the fragments. Formation of protonated $^{\gamma}[PD–H_2O]^{H+}$, the counterpart of $^{\gamma}[P_2D_3]^{H+}$, has the same *m/z* as $^{b}[PD–H_2O]^{ox+}$ because they are isomers. The γ-hydrogen and amide rearrangements can therefore not be distinguished with these fragment ions.

The rearrangement of the amide and ester bonds appears at approximately the same collision energy of $E_{kin,com}=0.6$ eV. The ions resulting from the loss of two H_2O molecules and the fragments due to rearrangement of the amide and ester bonds with an additional loss of H_2O appear, as observed for the other polymers, at a higher collision energy of 0.95–1.75 eV. The fragment $^{\gamma}[P_2D_3]^{H+}$ appears at the same collision energy as the fragments due to ester and amide bond rearrangement indicating that γ-hydrogen and ester/amide rearrangements of $[P_3D_4]^{H+}$ have similar activation energies.

The survival yield of parent ions $[G_3D_4]^{H+}$, $[S_3D_4]^{H+}$, $[C_3D_4]^{H+}$, and $[P_3D_4]^{H+}$ were compared by determination of the survival yield when 50% of the parent ion, indicative for the mean of the internal energy distribution, has fragmented. The 50% survival yield is observed for all parent ions at approximately 0.8 eV center of mass collision energy. This is because all polymers show similar fragmentation behavior since the amide and ester bonds are rearranged by the same mechanisms leading to similar fragments (oxazolonium ions).

3.4. Origin of the oligomeric ion series $P_3D_4–H_2O$, $S_3D_4–H_2O$, $G_3D_4–H_2O$, and $C_3D_4–H_2O$

The observations described in the previous paragraphs show that the lowest energetic fragmentation pathway observed for the hyperbranched polymers is the loss of H_2O. Nozzle skimmer activation in the ESI source will most likely lead to a loss of H_2O or an amide and ester rearrangement to oxazolonium ions. Two MS^n experiments are performed to determine whether the oligomeric ion series $P_3D_4–H_2O$, $S_3D_4–H_2O$, $G_3D_4–H_2O$, and $C_3D_4–H_2O$ observed in the mass spectra (see Fig. 2 for the phthalic acid anhydride based polymer) are formed during the polymerization process or as a result of in-source fragmentation processes. The first experiment is an MS^3 experiment where MS/MS of protonated $[P_3D_4]^{H+}$ is followed by CAD of the isolated oxazolonium fragment $[P_3D_4–H_2O]^{ox+}$. The latter MS/MS step of fragment $[P_3D_4–H_2O]^{ox+}$ is expected to show a different fragmentation behavior as observed for protonated species because the oxazolonium ion is not protonated. The second experiment is MS^2 of the oligomer $P_3D_4–H_2O$. If the oligomer is formed during the polymerization process it will appear as a protonated species in the mass spectrum $[P_3D_4–H_2O]^{H+}$. When the oligomeric ion is the result of in-source fragmentation, the ion is already a fragment ion and will appear in the mass spectrum as the oxazolonium ion $[P_3D_4–H_2O]^{ox+}$ with the same elemental composition as $[P_3D_4–H_2O]^{H+}$. The origin of the $P_3D_4–H_2O$ oligomer series can be determined by comparison of the MS^3 spectrum of the oxazolonium ion $[P_3D_4–H_2O]^{ox+}$ obtained from the MS^2 spectrum of $[P_3D_4]^{H+}$ with the MS^2 spectrum of $[P_3D_4–H_2O]^{H+}$ or $[P_3D_4–H_2O]^{ox+}$. The same set of experiments was also performed on parent ions S_3D_4, G_3D_4, and C_3D_4.

In Fig. 6 the MS^3 spectrum of $[P_3D_4–H_2O]^{ox+}$ obtained from MS^2 of $[P_3D_4]^{H+}$ (Fig. 5) is presented. The MS^3 spectrum contains fragment ions, which can all be explained by γ-hydrogen rearrangements. Note that rearrangements of the amide and ester bonds to oxazolonium ions are not possible, because free protons are not available. Most interesting about Fig. 6 is the absence of a fragment due to the loss of a H_2O molecule, which would have resulted in a fragment $[P_3D_4–2H_2O]^{ox+}$. The loss of H_2O has been observed for all protonated parent ions in Sec.3.3.

In Fig. 7, the MS^2 spectrum of $[P_3D_4–H_2O]^{H+}$ or $[P_3D_4–H_2O]^{ox+}$ is presented. Two important differences with Fig. 6 are observed. First, an intense loss of H_2O is observed resulting in fragment $[P_3D_4–2H_2O]^{ox+}$, which is not observed in Fig. 6. This indicates that the parent ion must be protonated. Subsequently, fragment $[P_2D_3]^{H+}$ is observed in Fig. 7 but not in the MS^3 data of $[P_3D_4–H_2O]^{ox+}$ obtained from MS^2 of $[P_3D_4]^{H+}$. Only a γ-hydrogen rearrangement of the ester bond of a protonated parent ion

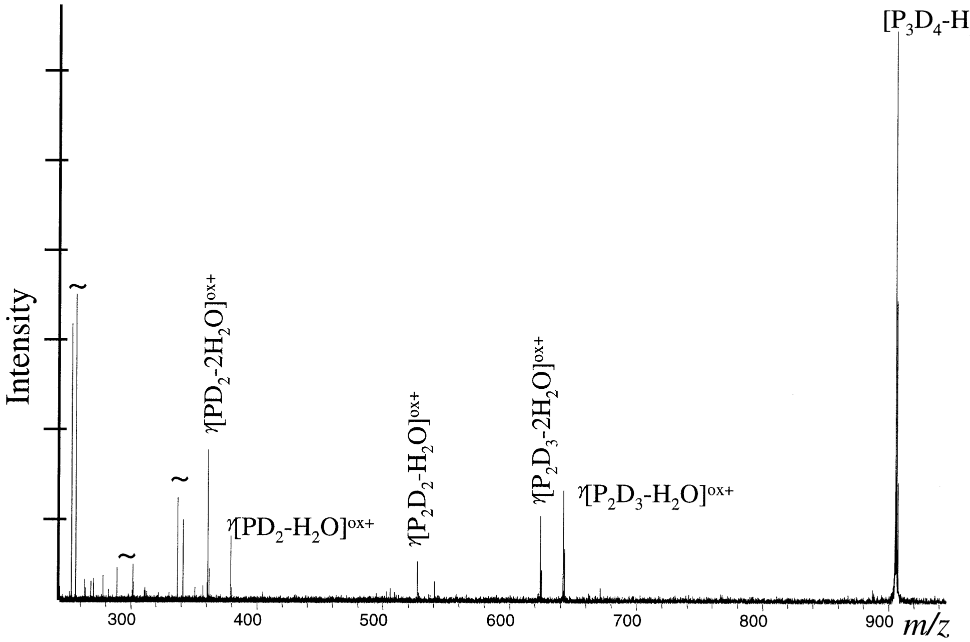

Fig. 6. MS^3 spectrum of the oxazolonium ion $[P_3D_4–H_2O]^{ox+}$ obtained from MS^2 from $[P_3D_4]^{H+}$ (Fig. 5). $E_{kin,com}(MS^2)=1.1$ eV, $E_{kin,com}(MS^3)=1.1$ eV.

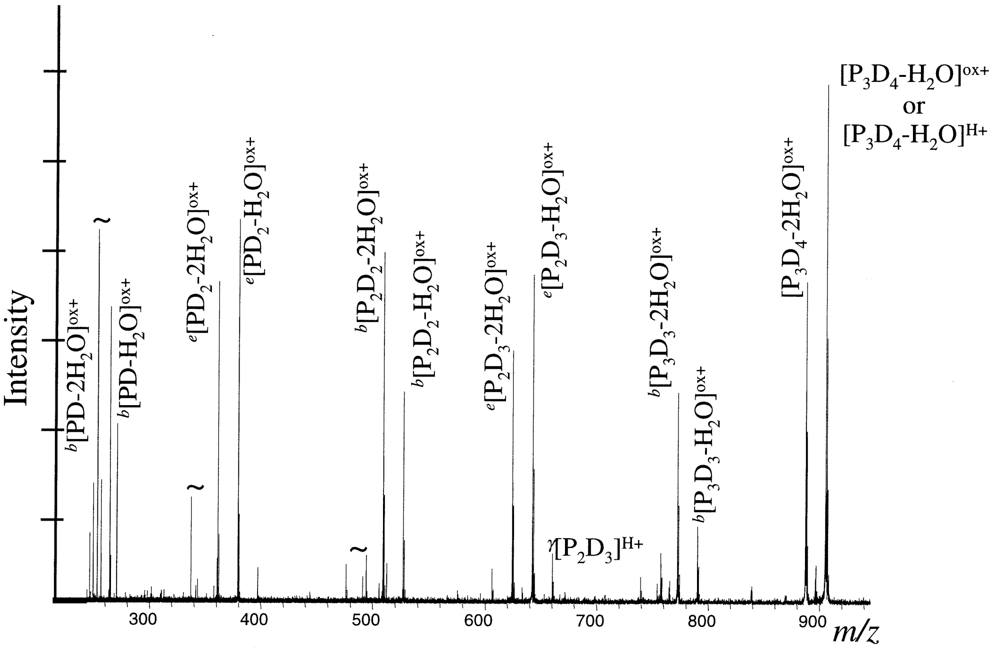

Fig. 7. MS^2 of $[P_3D_4–H_2O]^{ox+}$ or $[P_3D_4–H_2O]^{H+}$ at $E_{kin,com}=1.1$ eV.

$[P_3D_4–H_2O]^{H+}$ can explain the formation of this fragment, this is because the positive charge on the oxazolonium ion is fixed which must result in fragment $[P_2D_3–H_2O]^{ox+}$. For the protonated species a rearrangement of the ester bond leads to fragment $^{\gamma}[P_2D_3]^{H+}$. With the exception of γ-hydrogen rearrangements, the same fragmentation behavior has been observed for the other parent ions.

The observations described previously show that some of the fragments observed for MS^2 of $[P_3D_4–H_2O]^{H+}$ can not be formed by MS^2 of $[P_3D_4–H_2O]^{ox+}$, which demonstrates that the oligomeric ion series $P_3D_4–H_2O$, $S_3D_4–H_2O$, $G_3D_4–H_2O$, and $C_3D_4–H_2O$ observed in the mass spectra are protonated parent ions and therefore must originate from the polymerization process. These findings have been confirmed with NMR and titration experiments that have revealed a very low concentration of allylic end groups in the MWD, which are assumed to be due to elimination processes for which ester bonds are rearranged [28]. The inset of Fig. 2 shows that oligomer $[P_3D_4–H_2O]^{H+}$ is present in a high intensity, approximately 20% of $[P_3D_4]^{H+}$. It is however not possible to quantify the contribution of the oligomer series $P_3D_4–H_2O$, $S_3D_4–H_2O$, $G_3D_4–H_2O$, and $C_3D_4–H_2O$ in the molecular weight distributions with ESI FTMS. A part of the oligomer series $P_3D_4–H_2O$, $S_3D_4–H_2O$, $G_3D_4–H_2O$, and $C_3D_4–H_2O$ can still originate from in-source fragmentation. Quantification of the polymer related species is difficult for two reasons. (1) Differences in ionization efficiency between $P_nD_{n+1}–H_2O$ and P_nD_{n+1} ions can exist but have not been quantified. Significant differences in ionization efficiency have for example been observed for mixtures of the homopolyesters poly(di-propoxylated bisphenol-A/adipic acid) and poly(di-propoxylated bisphenol-A/isophthalic acid) [29]. (2) The fact that fragments of $[P_3D_4–H_2O]^{H+}$ can be distinguished from the fragments of $[P_3D_4–H_2O]^{ox+}$ but not the other way around further complicates quantification. It is therefore possible to demonstrate the presence of protonated species i.e. the species are formed in the polymerization reaction but it is not possible to quantify them.

4. Conclusions

The fragmentation behavior of a series of hyperbranched polyesteramides made by the polycondensation of the trifunctional diisopropanolamine (D) with the difunctional anhydrides of succinic acid (S), glutaric acid (G), 1,2-cyclohexane dicarboxylic acid (C), and phthalic acid (P) was studied by ESI FTMS. The breakdown diagrams of parent ions $[G_3D_4]^{H+}$, $[S_3D_4]^{H+}$, $[C_3D_4]^{H+}$, and $[P_3D_4]^{H+}$ were constructed using energy resolved on-resonance collisionally activated dissociation in the FTMS. Three main fragmentation pathways were observed that could be distinguished by the onset center of mass collision energy. The lowest energetic fragmentation pathway is the loss of H_2O leading to oxazolonium ions. The rearrangements of the ester and amide bonds, also leading to oxazolonium ions, were observed at higher onset collision energy. The loss of a second H_2O is observed at highest onset energies and most probably results in fragments with allylic or 2,6-dimethyl morpholine end groups.

The origin of an oligomeric ion series $P_3D_4–H_2O$, $S_3D_4–H_2O$, $G_3D_4–H_2O$, and $C_3D_4–H_2O$ observed in the mass spectra is determined with MS^n experiments. By comparing MS^3 experiments of $[P_3D_4–H_2O]^{ox+}$ obtained from the MS/MS of $[P_3D_4]^{H+}$ with MS^2 experiments of $P_3D_4–H_2O$, it was concluded that $P_3D_4–H_2O$ is present in the polymer sample. An intense loss of H_2O was observed from MS^2 of $[P_3D_4–H_2O]^{H+}$ but not from MS^3 of the oxazolonium ion $[P_3D_4–H_2O]^{ox+}$ obtained from the MS/MS of $[P_3D_4]^{H+}$. This demonstrates that $P_3D_4–H_2O$ is formed during the polymerization reaction leading to protonated species upon Electrospray Ionization. This phenomenon was observed for all four hyperbranched polyesteramides. The oligomeric ion series $P_3D_4–H_2O$, $S_3D_4–H_2O$, $G_3D_4–H_2O$, and $C_3D_4–H_2O$ are probably due to the formation of allylic end groups. This partly terminates the polymerization reaction, which influences the composition of the molecular weight distribution. These findings have been confirmed with NMR and titration experiments.

Acknowledgements

This work is part of the research program no. 28 “Mass Spectrometry of Macromolecular systems” of the “Stichting voor Fundamenteel Onderzoek der Materie (FOM)” a subsidiary of the “Nederlandse organisatie voor Wetenschappelijke Onderzoek (NWO)”. This project is financially supported by FOM, DSM Research (Geleen, The Netherlands) and Akzo Nobel Chemicals Research Arnhem (Arnhem, The Netherlands). The management of DSM Research, DSM Coating Resins, and DSM New Business Development is kindly acknowledged for granting the permission to publish this work. The authors would like to thank Dr. Xinghua Guo for useful discussions.

References

[1] P.O. Danis, D.E. Karr, F. Mayer, A. Holle, C.H. Watson, Org. Mass Spectrom. 27 (1992) 843.

[2] P.M. Lloyd, K.G. Suddaby, J.E. Varney, E. Scrivener, P.J. Derrick, D.M. Haddleton, Eur. Mass Spectrom. 1 (1995) 293.

[3] P.B. O’Connor, F.W. McLafferty, J. Am. Chem. Soc. 117 (1995) 12826.

[4] M.W.F. Nielen, Rapid Commun. Mass Spectrom. 10 (1996) 1652.

[5] G.J. van Rooij, M.C. Duursma, C.G. de Koster, R.M.A. Heeren, J.J. Boon, P.J. Schuyl, E.R.E. van der Hage, Anal. Chem. 70 (1998) 843.

[6] G. Wilczek-Vera, Y. Yu, K. Waddell, P.O. Danis, A. Eisenberg, Rapid Commun. Mass Spectrom. 13 (1999) 764.

[7] C.G. de Koster, M.C. Duursma, G.J. van Rooij, R.M.A. Heeren, J.J. Boon, Rapid Commun. Mass Spectrom. 9 (1995) 957.

[8] G.J. van Rooij, M.C. Duursma, R.M.A. Heeren, J.J. Boon, C.G. de Koster, J. Am. Soc. Mass Spectrom. 7 (1996) 449.

[9] S. Koster, M.C. Duursma, J.J. Boon, R.M.A. Heeren, J. Am. Soc. Mass Spectrom. 11 (2000) 536.

[10] A.T. Jackson, J.H. Scrivens, W.J. Simonsick, M.R. Green, R.H. Bateman, Proceedings of the 47th ASMS Conference on Mass Spectrometry and Allied Topics. Dallas, TX, 13–17 June 1999, p. 713.

[11] K. Urakami, N. Akimoto, K. Nishijima, Y. Kitanaka, M. Echigoya, K. Hashimoto, Chem. Pharm. Bull. 47 (1999) 1068.

[12] S. Koster, M.C. Duursma, J.J. Boon, M.W.F. Nielen, C.G. de Koster, R.M.A. Heeren, J. Mass Spectrom. 35 (2000) 739.

[13] S.M. Hunt, M.R. Binns, M.M. Sheil, J. Appl. Polym. Sci. 56 (1995) 1589.

[14] J.K. Gooden, M.L. Gross, A. Mueller, A.D. Stefanescu, K.L. Wooley, J. Am. Chem. Soc. 120 (1998) 10180.

[15] D. Muscat, H. Henderickx, G. Kwakkenbos, R. van Benthem, C.G. de Koster, R. Fokkens, N.M.M. Nibbering, J. Am. Soc. Mass Spectrom. 11 (2000) 218.

[16] J.W. Leon, J.M.J. Fréchet, Polym. Bull. 35 (1995) 449.

[17] H.S. Sahota, P.M. Lloyd, S.G. Yeates, P.J. Derrick, P.C. Taylor, D.M. Haddleton, J. Chem. Soc., Chem. Commun. (1994) 2445.

[18] R.A.T.M. van Benthem, N. Meijerink, E. Geladé, C.G. de Koster, D. Muscat, P.E. Froehling, P.H.M. Hendriks, C.J.A.A. Vermeulen, T.J.G. Zwartkruis, Macromolecules, to be published.

[19] In [15] the notation A is used for diisopropanolamine and D for 1,2-cyclohexane dicarboxylic acid anhydride. In this article we used a notation which is consistent with [18]. D is used to denote diisopropanolamine and C for 1,2-cylohexane dicarboxylic acid anhydride.

[20] R.M.A. Heeren, C.G. de Koster, J.J. Boon, Anal. Chem. 67 (1995) 3965.

[21] R.M.A. Heeren, J.J. Boon, Int. J. Mass Spectrom. Ion Processes 157/158 (1996) 391.

[22] R.M.A. Heeren, M.C. Duursma, L. Drahos, K. Vékey, Proceedings of the 48th ASMS Conference and Allied Topics, Long Beach, CA, 11–15 June 2000, p. 804.

[23] R.M.A. Heeren, K. Vékey, Rapid Commun. Mass Spectrom. 12 (1998) 1175.

[24] E. Geladéé, N. Meijerink, R. van Benthem, H. Henderickx, C.G. de Koster, Proceedings of the 48th ASMS Conference and Allied Topics, Long Beach, CA, 11–15 June 2000, p. 1520.

[25] D.G. Morgan, M.M. Bursey, Org. Mass Spectrom. 29 (1994) 354.

[26] M.J. Nold, B.A. Cerda, C. Wesdemiotis, J. Am. Soc. Mass Spectrom. 10 (1999) 1.

[27] A.G. Harrison, I.G. Csizmadia, T.-H. Tang, Y.-P. Tu, J. Mass Spectrom. 35 (2000) 683.

[28] R.A.T.M. van Benthem, C.G. de Koster, private communication.

[29] S. Koster, M.C. Duursma, J.J. Boon, H.J.A. Philipsen, J.W. v. Velde, M.W.F. Nielen, C.G. de Koster, R.M.A. Heeren, Macromolecules, submitted.